

Climate has contrasting direct and indirect effects on armed conflicts

David Helman^{1,2,*}, Benjamin F. Zaitchik¹ and Chris Funk^{3,4}

¹Department of Earth and Planetary Sciences, Johns Hopkins University, Baltimore, Maryland, USA

²Currently at Department of Soil & Water Sciences, The Robert H. Smith Faculty of Agriculture, Food & Environment, Rehovot, and Advanced School for Environmental Studies, The Hebrew University of Jerusalem, Jerusalem, Israel

³Earth Resources Observation and Science Center, U.S. Geological Survey, Sioux Falls, South Dakota, USA

⁴Climate Hazards Center, University of California, Santa Barbara, Santa Barbara, California, USA

Contact information:

David Helman (corresponding author)

david.helman@mail.huji.ac.il

Benjamin F. Zaitchik

zaitchik@jhu.edu

Chris Funk

chris.funk@geog.ucsb.edu

Climate has contrasting direct and indirect effects on armed conflicts

David Helman^{1,2,*}, Benjamin F. Zaitchik¹ and Chris Funk^{3,4}

¹Department of Earth and Planetary Sciences, Johns Hopkins University, Baltimore, Maryland, USA

²Currently at Department of Soil & Water Sciences, The Robert H. Smith Faculty of Agriculture, Food & Environment, Rehovot, and Advanced School for Environmental Studies, The Hebrew University of Jerusalem, Jerusalem, Israel

³Earth Resources Observation and Science Center, U.S.G.S., Sioux Falls, South Dakota, USA

⁴Climate Hazards Center, University of California, Santa Barbara, Santa Barbara, California, USA

There is an active debate regarding the influence that climate has on the risk of armed conflict, which stems from challenges in assembling unbiased datasets, competing hypotheses on the mechanisms of climate influence, and the difficulty of disentangling direct and indirect climate effects. We use gridded historical conflict records, satellite data, and land surface models in a structural equation modeling approach to uncover the direct and indirect effects of climate on violent conflicts in Africa and the Middle East (ME). We show that climate–conflict linkages in these regions are more complex than previously suggested, with multiple mechanisms at work. Warm temperatures and low rainfall direct effects on conflict risk were stronger than indirect effects through food and water supplies. Warming increases the risk of violence in Africa but unexpectedly decreases this risk in the ME. Furthermore, at the country level, warming decreases the risk of violence in most West African countries. Overall, we find a non-linear response of conflict to warming across countries that depends on the local temperature conditions. We further show that magnitude and sign of the effects largely depend on the scale of analysis and geographical context. These results imply that extreme caution should be exerted when attempting to explain or project local climate-conflict relationships based on a single, generalized theory.

1. Introduction

Although there is a suggested linkage between violent conflict and climate, the underlying mechanisms of the link are still under debate^{1,2}. One commonly suggested mechanism is of climate–conflict link through economic disruption^{3,4}. Though plausible, there is currently no robust evidence for such a direct climate–economy–conflict nexus⁵. Instead, many studies suggest that climate-driven depressions may lead to conflict through a combination of socioeconomic and political failure, particularly in agricultural dependent regions where people depend directly on such resources⁴. That is, climate influences economy, which influences social and political systems relevant to conflict.

It is also possible that the climate–conflict connection is less direct, operating through the influence that climate-induced changes in economy, food security, or group interactions cascade to influence the probability of inter-group violent conflicts. This indirect influence is relevant to theories like the “engagement” hypothesis, which claims that when climate crisis reduces economic productivity people become more likely to engage in conflicts than in economic activities^{6,7}, or the “inequality” hypothesis, which argues that conflict may upsurge when climate crisis increases economic inequality because of increasing efforts to redistribute assets⁸, and the “state weakness” hypothesis that suggests a weakening of governmental

45 institutions and their ability to suppress violence due to decline in economic productivity
46 following climate crisis⁹, all suggest that climate has an indirect, rather than a direct, effect
47 on violent conflicts¹⁰.

48 While these hypotheses were first studied in the context of civil wars and other state-
49 engaged conflicts, research in the past decade on communal, non-state violence has also
50 emphasized the mediated pathways through which climate can influence conflict. This
51 includes the potential for harmful climate anomalies like drought to drive conflicts in times of
52 scarcity due to resource competition, lowered opportunity cost, or other mechanisms^{11,12}. But
53 it also includes the potential for beneficial climate anomalies to increase conflict due to rent
54 seeking or available resources to support violent activities during times of abundance^{13,14}.
55 Studies have also found that climate variability in either direction can lead to increased
56 conflict, due to the presence of multiple mechanisms driving conflict or to the presence of
57 qualitatively different categories of conflict^{15,16}.

58 The direct influence of climate on individual tendency toward violence may also play a
59 role. Warming, for example, has been shown to enhance violence through a direct
60 psychological mechanism [the General Aggression Model – GAM] by making people
61 uncomfortable and irritated¹⁷. Alternatively, warming may enhance violence in cooler
62 environments because warm, more favorable weather conditions lead to increased activity
63 and interaction between people [Routine Activity Theory - RAT], which may lead to more
64 opportunities for conflict¹⁸.

65 To assess climate impacts on violence and uncover whether the underlying mechanisms
66 are direct, indirect, or a combination of both, ‘non-climatic’ effects must be isolated. Some
67 studies do this by pooling data across locations and applying statistical models that control
68 for non-climatic factors explicitly. The climate influence is then examined through its partial
69 effect on violence^{19,20}. Other researchers argue that controlling for non-climatic factors
70 explicitly can absorb most of the climatic impact and, therefore, may result in an
71 underestimation of the climate effect²¹. For this reason, it is argued, pooling analysis across
72 sites is misleading, and climate effects should be studied by comparing each place with itself
73 in time rather than with other places. Studies using this site self-comparison approach have
74 reached more conclusive results regarding climate impacts on violence than cross-sectional
75 studies using explicit controls^{21,22}. The problem with this self-comparison approach,
76 however, is that it cannot identify underlying ‘universal’ mechanisms because the analysis is
77 conducted location-by-location rather than across locations²³.

78 To some extent, the contrasting results published in the literature is a reflection of that
79 disagreement²⁴, with this inconsistency leading to criticism of climate-conflict research.
80 Some researchers have claimed that the link between climate and conflict is unsupported by
81 the evidence²⁵. Furthermore, researchers have been accused of bias in their approach to the
82 problem^{26,27}. Yet, most experts do believe that climate has a significant effect on human
83 conflicts²⁸, though the generality of the links and the underlying mechanisms are yet to be
84 established.

85 Here we use a powerful assemblage of disaggregated data (table S1), which includes the
86 Uppsala Conflict Data Program (UCDP) conflict dataset²⁹ as well as climatic [temperature
87 and rainfall anomalies] and non-climatic [anomalies in water availability, Infant Mortality
88 Rates, agricultural yield, and economic welfare] datasets derived from satellites and land
89 surface models to test generalizability of climate-conflict relationships from national to
90 continental scale. To leverage the strengths of the two approaches – the site self-comparison
91 and the use of explicit controls in a cross-sectional analysis – and explore general
92 mechanisms, we make use of structural equation modeling [SEM]³⁰ in which non-climatic

93 factors are explicitly controlled while direct and indirect effects of climate – through the non-
94 climatic factors – are quantified in order to uncover the underlying mechanisms.

95 We choose to focus on non-state conflicts rather than civil wars because small-scale
96 conflicts are likely to be more sensitive to environmental and climatic changes^{19,28}. Also, we
97 focus on Africa and the Middle East [ME] because these two regions experienced a large
98 number of armed conflicts in the last three decades (Fig. 1A). Finally, we hypothesize that
99 comparing these two ethnically and culturally distinct, but yet geographically close regions
100 may reveal contrasting mechanisms.

101 **2. Data and Methods**

102 Armed Conflict Dataset

103 *The UCDP Geolocated Violent Conflict Dataset*

104 We used the most updated Georeferenced Event Dataset [GED] Global version 18.1
105 (2017) of the Uppsala Conflict Data Program [UCDP²⁹] for location-specific information on
106 armed conflicts in Africa and the ME. The GED.v18.1 is UCDP's most disaggregated data
107 set, covering individual events of organized violence as phenomena of lethal violence
108 occurring at a given time and place. Events are sufficiently fine-grained to be geo-coded
109 down to the level of individual villages, with temporal durations disaggregated to single,
110 individual days³¹. Conflicts used here are “non-state” conflicts, defined by UCDP as “the use
111 of armed force between two organized armed groups, neither of which is the government of a
112 state, which results in at least 25 battle-related deaths in a year”³¹. Information on specific
113 conflict is freely available at [www.ucdp.uu.se], and questions regarding the definitions used
114 by UCDP as well as the content of the dataset can be directed to that site. In the GED dataset,
115 each conflict has a unique identifier [conflict ID], while the start date is recorded as precisely
116 as possible with the level of precision for day, month and year indicated alongside
117 [“Startprec” variable in GED.v18.1].

118 For our analysis we used conflicts indicated with a “Startprec” level of at least 5 meaning
119 that “Day and month are assigned, year is precisely coded; day and month are set as precisely
120 as possible”. A violent event was defined as a coded event, which is unique in terms of
121 starting and ends dates, and is not a continuation or part of a previous event. All events were
122 first binned at a spatial resolution of 0.5° x 0.5° for African and ME regions by summing the
123 total number of events per grid per year. Events were assigned to a specific year by indicated
124 starting date. A layer of violent events by 0.5° per year was produced alongside another layer
125 with the sum of events for the entire period of 1990 – 2017 (Fig. 1A). Because we look for
126 effects on the risk of violent conflict outbreak, each layer was converted into a binary layer in
127 which each grid was assign a value of 1 for grids that experienced violence during this year,
128 or 0 for grids that did not experience violence. Although we had information on violence for
129 1990- 2017, we used only layers for years 1992 – 2012 in the SEM analysis because this was
130 the period in which we had a complete data set of climate and non-climate variables (see
131 below). We included Syria in our analysis, but excluded the years after 2010 because of the
132 poor information on violent events during the period of the Syrian civil war^{31,32}.

133 Climate Data

134 *Temperature anomaly*

135 We used monthly maximum temperatures from the newly derived Climate Hazards
136 center Infrared Temperature with Stations [CHIRTS] dataset³³. CHIRTS provides monthly
137 2-m maximum air temperatures at a high spatial resolution of 0.05° and a quasi-global

138 coverage [60°S-70°N] from 1983 to 2016. Temperature estimates are derived using a
139 combination of thermal imagery from a constellation of geostationary satellites, a high-
140 resolution climatology from the Climate Hazards Center's Tmax climatology, and in situ
141 monthly 2-m Tmax air temperature observations obtained from the Berkeley Earth and
142 Global Telecommunication System [GTS]. We used the temperature estimates from CHIRTS
143 because these were shown to be suitable for monitoring temperature anomalies and extremes
144 in data-sparse regions like Africa and the ME³³. The high spatial resolution temperature
145 estimates were averaged over 0.5° x 0.5° for the period of the analysis [1992-2012], and the
146 yearly anomaly was calculated per grid as z-score [the long-term mean annual temperature
147 was subtracted from the specific year mean temperature and divided by the standard
148 deviation].

149 *Rainfall anomaly*

150 For rainfall anomaly, we used the Climate Hazards group Infrared Precipitation with
151 Stations [CHIRPS] dataset, available at a high spatial resolution of 0.05°³⁴. This product is
152 quasi-global precipitation product with daily to seasonal time scales and a 1981 to near real-
153 time period of record. CHIRPS uses three main types of information: (1) global 0.05° rainfall
154 climatologies, (2) time-varying grids of satellite-based rainfall estimates, and (3) in situ
155 rainfall observations. CHIRPS is built on 'smart' interpolation techniques and high
156 resolution, long period of record estimates based on infrared Cold Cloud Duration [CCD]
157 observations as well as on satellite information, used to represent ungauged locations.
158 CHIRPS is very reliable in regions like Africa and the ME where most rainfall products fail
159 to accurately represent the high temporal and spatial variability in rainfall³⁵ due to the sparse
160 gauge network in this region³⁶.

161 We used CHIRPS monthly rainfall sums [from January to December] to assess the
162 annual rainfall anomaly for 1992 – 2012, calculated as z-scores [the long-term mean annual
163 rainfall subtracted from specific year rainfall sum, divided by the standard deviation]. Each
164 year a z-score map was produced while pixels were aggregated to the spatial resolution of the
165 analysis [0.5° x 0.5°]. Annual rainfall is not a comprehensive proxy for conflict-relevant
166 rainfall variability, but it offers a practical, objective measure that can be applied consistently
167 across our diverse study domain.

168 Non-Climate Data

169 *Infant Mortality Rate*

170 As a proxy of socioeconomic development, we used information on infant mortality rate
171 [IMR] from the Global Subnational Infant Mortality Rates, Version 1 [GSIMR.v1]³⁷. The
172 GSIMR.v1 dataset is produced by the Columbia University Center for International Earth
173 Science Information Network [CIESIN] at a high spatial resolution of 5 km and is freely
174 available for download as a raster data layer from [<http://www.ciesin.columbia.edu/povmap>].
175 The GSIMR.v1 consists of IMR estimates for the year 2000, which was collected from vital
176 registration data, surveys and models or estimated using reported live births and infant deaths
177 data. Though our analysis spans the period of 1992 – 2012, we assume that the 2000
178 GSIMR.v1 is, in average, representative of the entire period following previous studies³⁸.
179 The IMR is calculated as the number of deaths of infants of less than one year old divided by
180 the number of live births and multiplied by 1000. We preferred using the IMR as a proxy of
181 poverty and socioeconomic status instead of using other variables because measures like
182 Gross Domestic Product [GDP] or population living on less than one U.S. dollar per day, are
183 difficult to obtain at sub-national levels, particularly for the regions of this study. Moreover,
184 using IMR has several advantages over other socioeconomic metrics. For example, IMR is a

185 highly standardized measure compared to other measures, which means that it can be used to
186 compare between countries with different economic systems better than GDP, for example ³⁸.
187 Also, IMR is less likely to be influenced by skewed wealth distribution. And, information on
188 IMR is available for ~90% or more of the population in medium and low-income countries.
189 The original 5-km IMR data layer was binned at the spatial resolution of 0.5° x 0.5°, which is
190 the resolution of the analysis and used as a static map layer.

191 *Distance to Border*

192 Distance from/to political borders was assessed using a geographical information system
193 and a shapefile layer of the political borders of African and the ME countries. The minimal
194 distance from each grid cell to the nearest border was recorded and used in the SEM analysis.
195 Because this information is static [i.e., it does not change during the period of analysis] the
196 same value was used in all years.

197 *Agricultural Dependence*

198 To assess agricultural dependence as share of cropland area in a 0.5° grid cell, we used
199 the Climate Change Initiative [CCI] of the European Space Agency [ESA] Land Cover
200 product. The ESA CCI product is an annual global land cover time series from 1992 to 2015
201 [now available also for 2016 to 2018], available at an unprecedented high spatial resolution of
202 300 m (<https://www.esa-landcover-cci.org/?q=node/175>). This unique dataset was produced
203 by reprocessing and interpretation of daily surface reflectance of five different satellite
204 missions. It uses the full archive of MERIS [2003–2012], with 15 spectral bands and 300 m
205 spatial resolution and the 1 km time series from AVHRR [1992–1999], SPOT-VGT [1999–
206 2013] and PROBA-V [2014 and 2015]. The baseline was established through MERIS data
207 and use of machine learning and unsupervised algorithms ³⁹.

208 The advantage of this product over other products that are derived from several
209 observation systems is that it maintains a good consistency over time. This is done by
210 confirming changes observed in earlier and later MERIS era satellites via back- and forward
211 checking through the 10-year MERIS base-line LC maps. The ESA CCI LC product was
212 evaluated with a global independent validation dataset according to international standards,
213 testing the accuracy of both LC classes and LC change in time ³⁹. It was also found accurate
214 through a comparison using country-level information provided by the Food and Agriculture
215 Organization of the United Nations [FAO-STAT] in several countries ⁴⁰.

216 We used the 1992 – 2012 ESA CCI LC maps to classify pixels into agricultural *versus*
217 non-agricultural classes. More specifically, LC classes #10, 20, 30, and 40, which include
218 also mosaics of croplands and natural vegetation, were designated as agricultural pixels while
219 others were assigned as non-agricultural pixels. We then aggregated the 300-m pixels into the
220 coarser resolution of 0.5° [resolution of analysis] and calculated the total share of agricultural
221 area in each 0.5° grid cell [as the percentage of total area]. These estimates were used to
222 examine influence of agricultural dependence [larger crop share of area equals higher
223 agricultural dependency ³⁸] on violence risk as well as to derive yearly change in agricultural
224 yield production [see next sub-section].

225 *Yield Production*

226 To quantify changes in agricultural yield production, we used NASA's VIPPHEN EVI2
227 satellite product ⁴¹. The VIPPHEN EVI2 data product is provided globally at 0.05° [~5600
228 meters] spatial resolution and contains 26 Science Datasets [SDS], including phenological
229 metrics such as the start, peak, and end of season as well as the maximum, average, and
230 background calculated EVI2 (https://lpdaac.usgs.gov/products/vipphen_evi2v004/). It is

231 currently the longest and most consistent satellite-based global vegetation phenology product
 232 available. VIPPHEN SDS are based on the daily VIP product series and are calculated using
 233 a 3-year moving window average to eliminate noise.

234 The modified 2-band enhanced vegetation index [EVI2] is highly correlated with the
 235 commonly-used EVI⁴², which was found to be useful for tracking changes related to
 236 vegetation dynamics⁴³ as well as gross primary productivity⁴⁴. EVI2 differs from the
 237 traditional EVI by its use of two bands, the red and near infrared, instead of the use of three
 238 bands, which includes also the blue band in the index calculation. The integral over the
 239 growing season of EVI2 [EVI_{GSI}; fig. S1] was used here as a proxy of agricultural yield
 240 production. Growing season integrals of vegetation indices are usually well correlated with
 241 biomass of green tissues, particularly in annual vegetation systems^{45–47}, and as such may
 242 serve as a good proxy of crop yield production⁴⁸. EVI_{GSI} was derived per year for
 243 agricultural pixels with > 50% of agricultural area cover [estimated from the ESA CCI LC
 244 300 m product]. Pixels with < 50% of agricultural area cover were discarded from the
 245 analysis in order to remove influences of non-agricultural vegetation systems on EVI_{GSI}.

246 Because agricultural fields differ in crop type and different crop types may have similar
 247 EVI_{GSI} values, we used the relative anomaly of EVI_{GSI} as a proxy of relative anomaly in local
 248 yield production instead of the absolute EVI_{GSI} value. In order to assess the validity of this
 249 approach, we compared yearly anomalies of national yield production, derived from the food
 250 and agriculture data provided by the Food and Agriculture Organization of the United
 251 Nations [FAO-STAT⁴⁹], with country-level EVI_{GSI} anomalies (z-scores) for the period of
 252 analysis [1990–2012; see *Supplementary Material* and figs. S2 to S5]. Yield is provided in
 253 FAO-STAT as hectograms per hectare [hg/ha] for cereals, citrus fruit, coarse grain, fibre
 254 crops, oil-crops, pulses, roots and tubers, treenuts, vegetables and fruits
 255 (<http://www.fao.org/faostat/en/#data/QC>). The total annual yield and the long-term mean
 256 annual yield [1990–2012] from FAO-STAT were calculated to derive the relative anomaly in
 257 percentages of the long-term average yield [%]. The same procedure was applied for the
 258 calculation of the EVI_{GSI} annual anomaly [as percentages of the mean EVI_{GSI}].

259 *Satellite Night-time Lights as A Proxy of Economic Welfare*

260 We used night-time lights intensity from the Defense Meteorological Satellite Program
 261 [DMSP⁵⁰] to estimate grid-based economic welfare status and dynamics in Africa and the
 262 ME. This night-time light product dates back to 1992 and is considered to be well correlated
 263 with GDP, built-up area, energy consumption, poverty, and other socioeconomic welfare
 264 variables^{51–54}. We used the DMSP yearly average stable night-time lights intensity product at
 265 a spatial resolution of 30 arcsec [~1km] for 1992–2012 to calculate the percentage area of
 266 light per pixel [LitArea]. Method was followed by the described in⁵⁵. In short, light intensity
 267 in DSMP is given as a digital number [DN] from 0 to 100 for each pixel. A DN threshold
 268 value is then used to assign each pixel with a binary 1/0 for presence/absence of light. The
 269 threshold of DN>31 was used following⁵⁵. The total LitArea per 0.5° grid – i.e. the sum of
 270 the squared kilometers of light in a 0.5° grid cell – was derived by aggregating pixels with
 271 values to the spatial resolution of the analysis. The total number of square kilometers was
 272 then converted into square meters and divided by the population density in the same grid cell
 273 to derive the relative LitArea [R-LitArea].

274 This was done because places with denser populations are expected to have higher
 275 LitArea, which will not necessarily indicate a higher economic welfare status but may just
 276 reflect a larger build-up area. By dividing the LitArea by the population density, we thus
 277 normalize for such an effect, remaining with a relative measure of economic welfare. We
 278 used the WorldPop dataset [www.worldpop.org.uk] for grid-based information on population

279 density. This dataset uses an ensemble learning method for classification, combining 30-m
 280 Landsat Enhanced Thematic Mapper (ETM) satellite imagery for high-resolution mapping of
 281 settlements and gazetteer population numbers to produce gridded population density maps at
 282 high spatial resolutions⁵⁶. Yearly population maps for Africa and the ME are available from
 283 2000 to date [downloaded from: <https://www.worldpop.org/project/categories?id=3>] at the
 284 same resolution of the DMSP dataset [1km x 1km]. We used simple linear interpolation to
 285 derive population density for 1992-1999, and aggregated the original resolution to the coarse
 286 spatial resolution of the analysis [0.5° x 0.5°]. R-LitArea was derived per 0.5° grid cell as the
 287 ratio between LitArea and population density. Finally, R-LitArea z-score was calculated to
 288 get yearly economic welfare anomaly.

289 *Grid-Based Water Resources Information from Land Surface Models*

290 Gridded estimates of soil moisture and hydrological fluxes, along with river network
 291 estimates of streamflow, were generated using the NASA Land Information System [LIS]⁵⁷
 292 software frameworks. In this implementation, LIS was implemented using the Noah-
 293 MultiParameterization [Noah-MP]⁵⁸ Land Surface Model and the Hydrological Modeling
 294 and Analysis Platform [HyMAP]⁵⁹ river routers. All simulations were performed using
 295 meteorological forcing data drawn from the NASA Modern Era Reanalysis for Research and
 296 Applications, v2 [MERRA-2]⁶⁰, with the exception of precipitation, which came from the
 297 Climate Hazards InfraRed Precipitation with Stations, v2 [CHIRPSv2]³⁴ dataset. Simulations
 298 were performed at 0.1° horizontal resolution with a timestep of 30 minutes. A 30-year spin-
 299 up was performed to equilibrate model soil moisture states, and the simulation was then run
 300 from 1990-2018. In this application, Noah-MP was used with four soil moisture layers
 301 [thicknesses of 0.1, 0.3, 0.6 and 1.0 m, descending from the surface] and a simple unconfined
 302 aquifer. Soil moisture and surface runoff were aggregated to the spatial resolution of the
 303 analysis and the z-score of each 0.5° grid cell was calculated to derive the inter-annual
 304 anomaly.

305 **4. Assessing Direct and Indirect Causal Effects**

306 The SEM approach was used because it allows to evaluate direct and indirect effects of
 307 climate and non-climate factors on violence risk, as well as to quantify relationships among
 308 factors. In that sense, SEM has an advantage over univariate regression approaches, such as
 309 general additive models (GAM) and general linear models (GLM), because it can be used to
 310 evaluate direct effects while controlling for joint effects. For example, it provides a way to
 311 evaluate the direct effect of yield on conflict risk while controlling for the joint effects of
 312 climate variables on yield and conflict. The ability of SEM to quantify direct and indirect
 313 relationships makes it particularly suited for confirming causal relationships based on *a priori*
 314 hypotheses.

315 Our SEM was developed based on a conceptual model designed to test *a priori*
 316 hypothesis that relates climate to food and water security, economic welfare and – directly
 317 and indirectly – to conflict risk⁶⁻⁹. It was then applied on a 0.5° grid basis in a time-for-space
 318 model design for 1992-2012 (see *Supplementary Material*). The SEM model was applied for
 319 Africa, the ME, and both regions together, as well as for each country separately. To enable
 320 comparison between datasets with different normal distributions, we used the relative
 321 anomaly – quantified as a standard score [z-score] – instead of the absolute values of the
 322 climate and non-climate factors. The control variables [IMR, agricultural dependence and
 323 distance to border], on the other hand, were maintained with their absolute values in order to
 324 quantify the absolute influence of these factors on the climate-conflict relationships. The

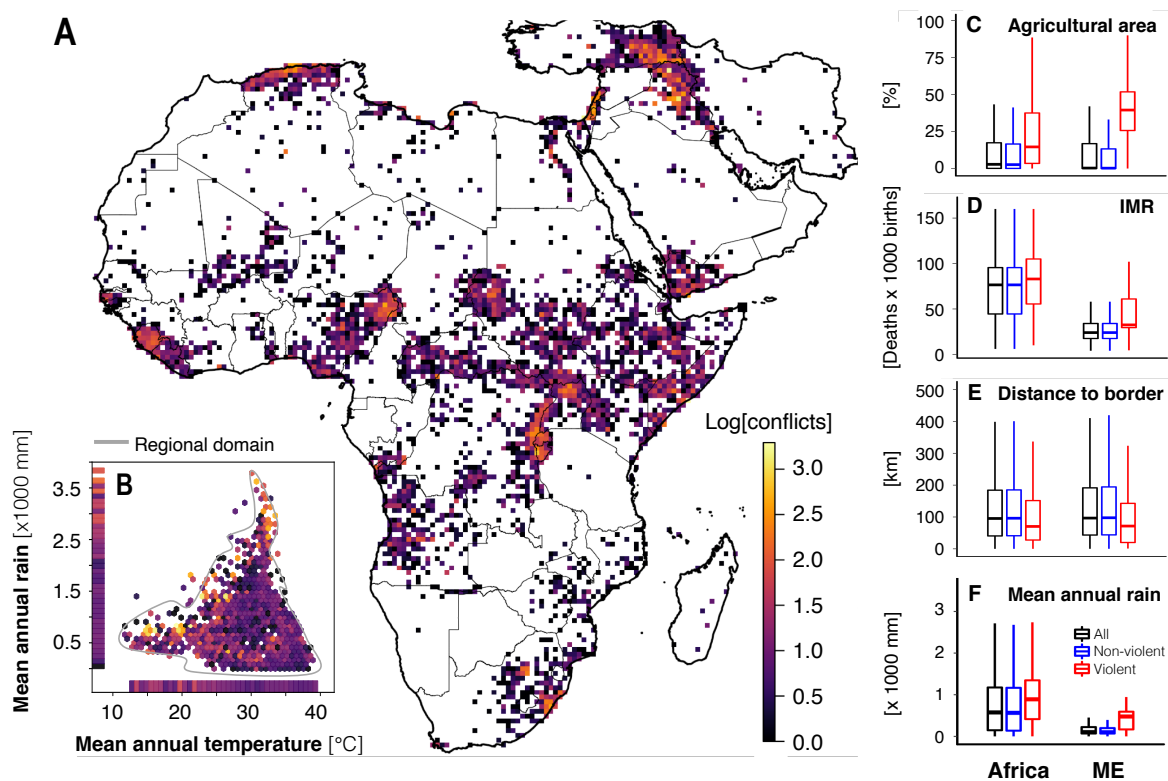
325 conflict data was converted to a binary dataset, with 0 for non-conflict and 1 for conflict
 326 years/grids.

327 The results of the SEM are presented as standardized effects indicating the magnitude
 328 and sign of effect.

329 5. Results and Discussion

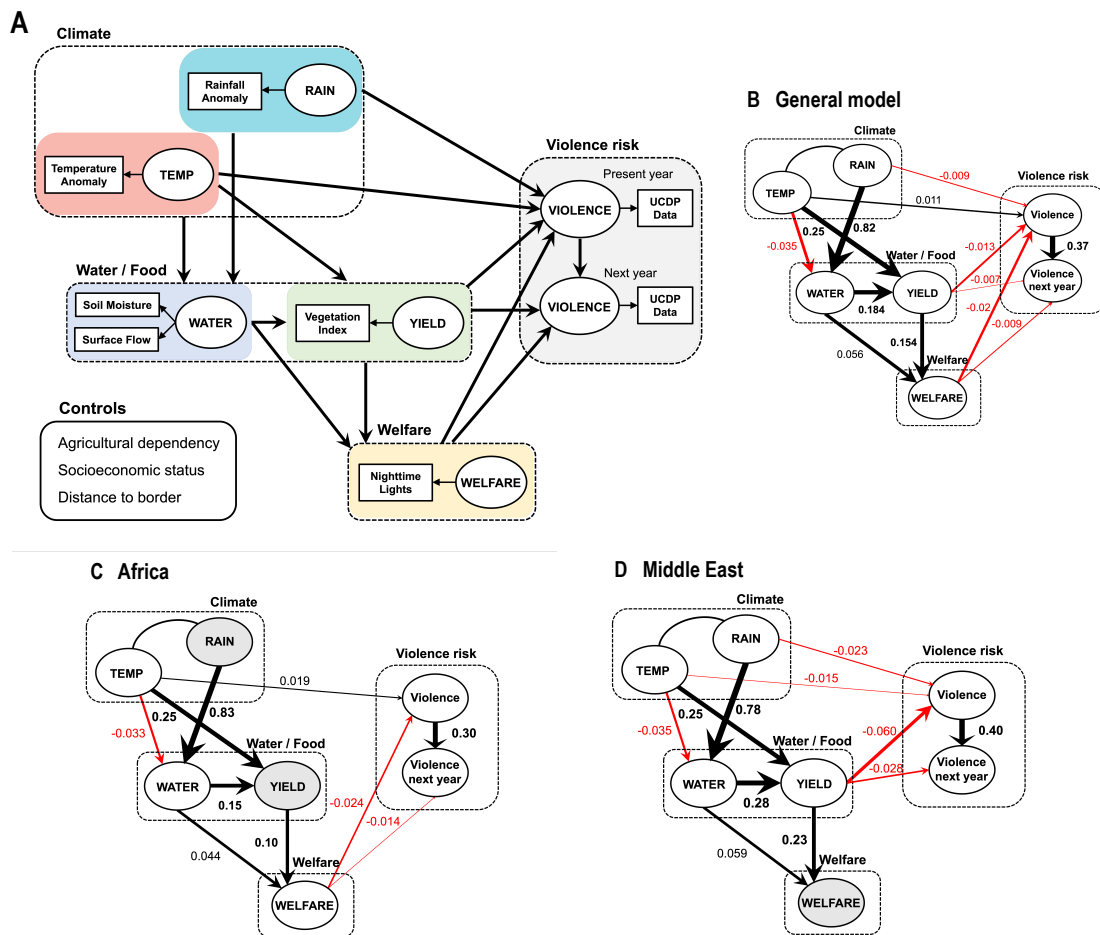
330 Armed conflicts in the last three decades were not restricted to certain climatic conditions in
 331 Africa and the ME but rather occupied the entire climatic domain (Fig. 1B). Consistent with
 332 previous studies, conflicts are mostly found in agriculture dependent areas³⁸, low socio-
 333 economic areas⁶¹, and close to political borders¹⁹ in both regions (Fig. 1C to E).

334 Conflict grid cells also have higher than average rainfall (Fig. 1F) on account of the fact that
 335 population and agricultural activities are limited in arid regions. However, the association
 336 between violence and agricultural dependence was about four-fold stronger in the ME (Table
 337 1), in spite of the larger average agricultural area in Africa [14% compared to 11% for the ME]
 338 (Fig. 1C), likely because of lower mean annual rainfall and therefore greater agricultural
 339 vulnerability to drought and water scarcity (Fig. 1F).



340 **Figure 1. Armed conflicts in Africa and the Middle East, and associated factors.** (A) Log number of armed
 341 conflicts by 0.5° grids for 1990 – 2017. (B) Mean annual rainfall and temperature binned by log number of
 342 conflicts. Gray line in (B) marks the region’s climatic domain (95th quantile of all grids). Boxplots show median,
 343 1st and 3rd quantiles of (C) relative agricultural area, (D) infant mortality rate (IMR), (E) distance to border, and
 344 (F) mean annual rainfall for violent (red), non-violent (blue) and all (violent + non-violent) grids. Violent grids
 345 are significantly different from non-violent grids in (C to F) at $P < 0.001$.

346 **Contrasting Climate Effects in Africa and the Middle East.** When applying the SEM to
 347 both regions together [general model] (Fig. 2B), yield and economic welfare had the
 348 strongest effect on present-year violence risk. Increases in yield and welfare reduced the
 349 chance of violence in both present and following year, while warming increased the risk and
 350 rain decreased this risk.



351
 352 **Figure 2. Structural equation models showing causal effects on conflict risk.** (A) The conceptual model.
 353 Models were applied to (B) Africa and Middle East together (general model), and to (C) Africa and (D) Middle
 354 East separately. Factors not affecting present-year violence are colored gray. Numbers alongside arrows indicate
 355 the standardized direct effects, with the color of the arrow indicating its sign (black for positive; red for negative)
 356 and width indicating its importance in the model. Constructs in our SEM are indicated by ovals while indicators
 357 are shown as rectangles. Only significant effects at $P < 0.05$ are shown.

358 While these results are in accordance to previously reported by others^{19,21,38}, unexpected
 359 complex climate-conflict links were revealed when SEMs were applied to each region
 360 separately (Fig. 2C and D). Warming increased the risk of violence in Africa (Fig. 2C) –
 361 similar to the general model – but unexpectedly decreased this risk in the ME (Fig. 2D).
 362 There was no effect of rain and yield on conflict risk in Africa and no effect of welfare in the
 363 ME. But there was a weak, though significant ($P < 0.05$), indirect negative effect of rain on
 364 the risk of conflicts in Africa (Table 1), which was, surprisingly, through the effect of water
 365 availability on welfare and not through yield (Fig. 2C). This may be in part because satellite-
 366 based estimates of yield have limited skill in some conflict-prone African regions (fig. S3 and
 367 S4), but could also be due to a more complex link between rainfall, yield and violence than
 368 that drawn by our model. In all models, the risk of violence was greater in places were
 369 conflict already occurred in the previous year (Fig. 2B to D).

370 **Table 1.** Direct, indirect and total standardized effects of rain, temperature and yield anomalies on risk of violence,
 371 with and without explicit controls (marked in italic). High infant mortality rate (IMR) means low socio-economic
 372 status. Positive (negative) relationships are shown in black (red) font.

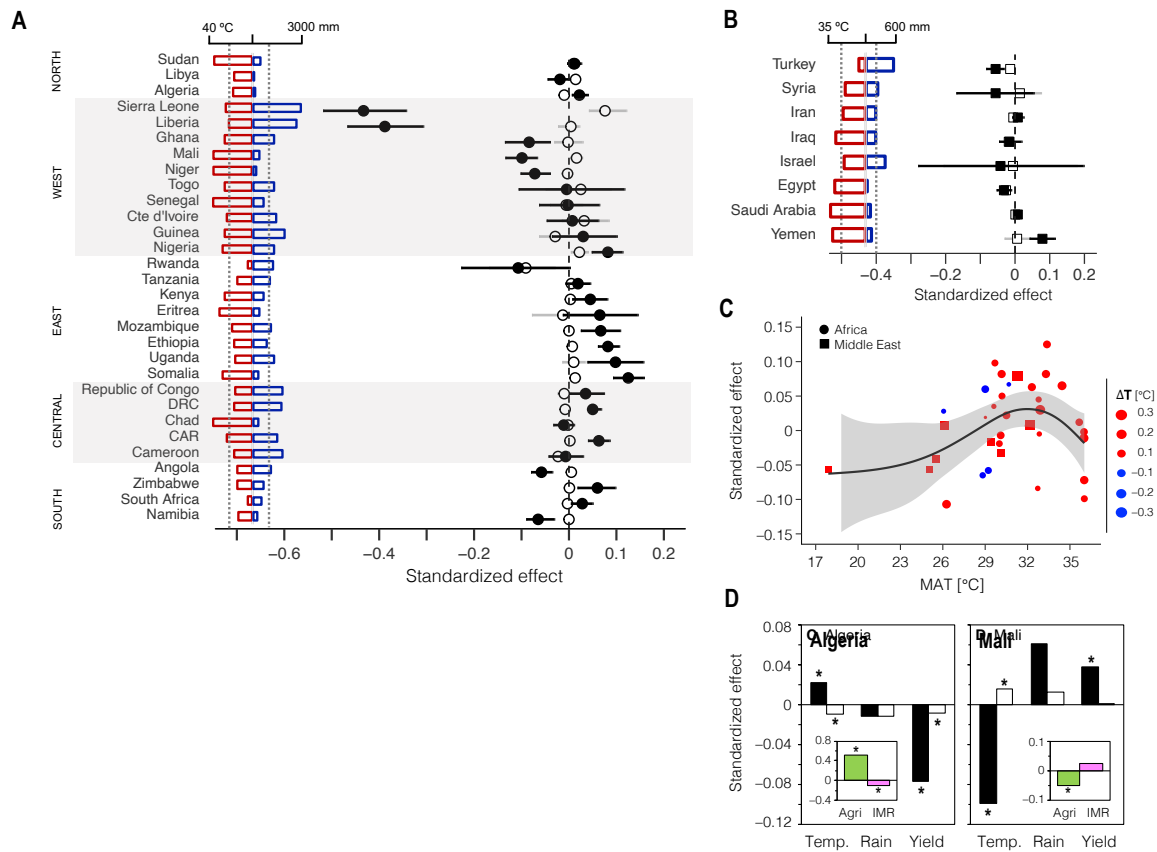
	Predictor	Without controls			With controls		
		Direct	Indirect	Total	Direct	Indirect	Total
General model	Rain	n.s.	-0.003**	-0.006**	-0.009**	-0.003**	-0.012**
	Temperature	0.011**	-0.003**	0.008**	0.011**	-0.004**	0.008**
	Yield	-0.009**	-0.003**	-0.013**	-0.013**	-0.003**	-0.016**
	<i>Agricultural area</i>	-	-	-	0.110**	-	-
	<i>IMR</i>	-	-	-	0.017**	-	-
	<i>Distance to border</i>	-	-	-	-0.033**	-	-
Africa	Rain	n.s.	n.s.	n.s.	n.s.	-0.001*	n.s.
	Temperature	0.020***	n.s.	0.020***	0.019**	n.s.	0.019**
	Yield	n.s.	-0.002***	n.s.	n.s.	-0.002**	n.s.
	<i>Agricultural area</i>	-	-	-	0.073**	-	-
	<i>IMR</i>	-	-	-	0.023**	-	-
	<i>Distance to border</i>	-	-	-	-0.030**	-	-
ME	Rain	-0.015**	-0.009***	-0.025***	-0.023**	-0.012**	-0.036**
	Temperature	-0.026***	-0.011***	-0.037***	-0.015**	-0.014**	-0.028**
	Yield	-0.048***	n.s.	-0.047***	-0.060**	n.s.	-0.058**
	<i>Agricultural area</i>	-	-	-	0.264**	-	-
	<i>IMR</i>	-	-	-	0.083**	-	-
	<i>Distance to border</i>	-	-	-	n.s.	-	-

n.s. not significant; * $P < 0.05$; ** $P < 0.01$; *** $P < 0.001$

374 **A Non-Linear Response of Conflict to Warming.** To examine the generality of the
 375 contrasting effects, we further applied the SEMs per country. After analyzing the countries
 376 with enough conflicts to produce a statistically significant model (table S4), we found that not
 377 only ME countries, but also some African countries – particularly West African – had a
 378 negative, direct temperature effect on violence risk (Fig. 3A). This is although some of these
 379 countries are warmer than those showing a positive effect [e.g. East African countries], which
 380 would theoretically make them more vulnerable to heat-induced violence²³. In general, the
 381 country data show a non-linear relationship between the warming effect – i.e. the
 382 standardized direct effect of temperature anomaly on conflict risk – and the mean temperature
 383 conditions across countries, with a peak response at around 32°C (Fig. 3C). Countries with
 384 lower and higher mean annual temperatures (MAT) tend to exhibit lower effects of
 385 temperature anomalies on the risk of violence, with even negative effects in some cases.

386 An example of the latter is Sierra Leone and Liberia, which had the strongest effects,
 387 with a standardized negative effect of -0.43 and -0.39, respectively (Fig. 3A). These two
 388 countries are characterized by extremely warm and humid conditions, with high temperatures
 389 and large amounts of rainfall year-round (~3000 mm y⁻¹). Contrary to the GAM, which
 390 suggests that uncomfortable environmental conditions increase violent perceptions³, in this
 391 case uncomfortable extreme weather conditions [extra warming in already warm, humid
 392 countries] seemed to decrease the risk of violence.

393 Though under debate, previous studies suggest that physical aggression may have a
 394 rather complex, curvilinear response to heat^{62–64}. Aggression was shown to increase with
 395 temperature rise, but decrease at excessive heat in several experimental settings, particularly
 396 when other negative-affect-producing factors are present⁶⁴. The explanation given for this is
 397 that it is the urgent ‘need’ to escape or minimize discomfort which overcomes tendencies to
 398 aggressive behavior⁶⁵. Taking this to Sierra Leone and Liberia, a further increase in
 399 temperature resulting in extremely unpleasant conditions might have increased discomfort
 400 and reduced the level of engaging in violence through such ‘escape’ mechanism. In this
 401 context, the RAT – suggesting that people interact more under pleasant conditions, which
 402 lead to more opportunities for violence – may be another possible explanatory mechanism¹⁸.



403

404 **Figure 3. Contrasting effects of temperatures on conflict risk.** Direct (close symbols) and indirect (open symbols) standardized effects of temperature on the risk of conflict from SEMs in (A) African and (B) Middle Eastern countries. Mean annual temperature and rainfall over 1992 – 2012 are shown. Effects with bars not crossing the vertical line in (A and B) are considered significant at $P < 0.05$. (C) The standardized direct effect of temperature vs. local temperature conditions expressed as the mean annual temperature [MAT]. Each symbol in (C) is a single country (Sierra Leone and Liberia are excluded for clarity), with the size indicating the average temperature change $[\Delta T]$ for the period of analysis and the line depicting the nonparametric regression with corresponding confidence interval. (D) The standardized direct (black) and indirect (white) effects of temperature, rain, and yield on conflict risk in Algeria and Mali. Inserts in (D) show the effects of agricultural dependence and infant mortality rate (IMR) in Algeria and Mali. Asterisks denote significant effects at $P < 0.05$.

414 The positive and negative temperature effects in Yemen and Turkey (Fig. 3B) suggest
 415 that GAM is the primary mechanism in the ME rather than the RAT. The contrasting sign
 416 effect may be explained by a relaxation mechanism in which a decrease in unpleasant
 417 conditions – being warming in a cold area [Turkey] or cooling in a warm area [Yemen] –
 418 reduces the chance of violence⁶⁶. This does not necessarily contradict the abovementioned
 419 ‘escape’ theory because warm and humid conditions in both Turkey and Yemen are more
 420 tolerable than in Sierra Leone and Liberia (Fig. 3A,B).

421 **Climate Effects in the Context of Geography and Ethnicity.** To further show how
 422 complex this climate-conflict link may be, we focus on two cases –Algeria and Mali. Algeria
 423 is the largest country in Africa, with an economy relying heavily on energy exports. Though
 424 Algeria’s government has promoted agricultural development, yield is highly unstable due to
 425 climate variability⁶⁷. This instability is likely to promote violence, particularly in agriculture
 426 dependent areas as shown from our results (Fig. 3D). The contrasting indirect [negative] and
 427 direct [positive] effects of temperature in Algeria are likely due to a positive temperature
 428 effect on yield and a direct adverse influence of heat, which may be explained by the GAM.

429 In contrast, the influence of yield on violence risk was positive and significantly smaller in
 430 Mali [50% smaller than in Algeria]. This is in spite of the fact that Mali's economy is more
 431 centered on agriculture than Algeria⁶⁸. Moreover, the positive yield effect was limited to the
 432 northern part of Mali, which is less agricultural than its southern [and central] part (insert in
 433 Fig. 3D).

434 Putting this in context, we know that most conflicts in Mali during the period of analysis
 435 were intra-state conflicts between the government and the Tuareg nomadic inhabitants living
 436 in the northern part of the country. Because our analysis is limited to small-scale conflicts,
 437 the non-state, inter-group aspects of the Tuareg conflict, which occur primarily in the
 438 northern, less agricultural part of the country, is well noted (Fig. 1A)⁶⁸. The Tuaregs are
 439 primarily pastoral and as such continuously compete for scarce resources between pastoral
 440 groups and with the few crop farmers and settled villagers in the north⁶⁸. Tuareg conflict is
 441 believed to be an example of a resource conflict driven by climatic changes⁶⁹ and the
 442 positive effect of yield on violence risk in our SEM is likely a reflection of this struggle, with
 443 periods of increased yield in the northern region being a potential driver of ethnic tension and
 444 inter-group violence.

445 These contrasting complex links in Algeria and Mali imply that the climate-violence
 446 linkage should be investigated in the context of historical, geographical and ethnical
 447 backgrounds of each location rather than as a general cross-sectional analysis. Such an
 448 approach can shed light on contrasting effects of climate.

449 **6. Concluding Remarks**

450 Our findings reveal previously unreported effects of climate on risk of conflict outbreak.
 451 More specifically, contrasting effects of temperature were detected at a regional scale and in
 452 numerous countries in Africa and the ME. Importantly, temperature and rainfall direct effects
 453 on conflict risk seem to be stronger than any indirect effect through resources such as water
 454 availability and agricultural production (Fig. 3 and Table 1). This could mean one of three
 455 things: that climate affects violence mostly through psychological and/or interactive
 456 mechanisms [e.g. GAM and RAT^{17,18}]; that indirect effects depend on aspects of climate
 457 variability that we have not considered⁷⁰; or that underlying mechanisms in which resource
 458 scarcity or conflict-relevant abundance patterns affect violence are more complex than those
 459 modeled by our SEMs.

460 As in previous studies²¹, the use of explicit controls affected the strength of the climate
 461 effect in our SEMs [i.e. the difference between total and direct effects in Table 1], in our case
 462 by up to 46%. This was important enough to expose indirect rain effects in Africa (Table 1).
 463 It is important to note that the SEMs, although statistically significant (table S4), confirming
 464 the validity of the a priori hypothesis, had very little predictive power [with 1st and 3rd
 465 quantiles being 1.6% and 11% across countries] (table S5). This means that although our
 466 SEMs did confirm impacts of climate on armed conflicts by effectively quantifying its direct
 467 and indirect effects, these effects were relatively small compared to unobserved factors like
 468 political, ethnic and likely other unaccounted socioeconomic factors. These were only partly
 469 considered in our analysis, due to the difficulty to account for such factors at a grid-cell level,
 470 in the form of next-year violence risk, which was shown to be greatly affected by present
 471 year violence (explaining between 10% and 16% of the variance, at the continental level; Fig.
 472 2B to D).

473 Our results demonstrate that no single proposed climate-conflict mechanism can alone
 474 explain the empirical patterns that underlie the climate-conflict linkage across contrasting
 475 regions or countries, and that this linkage is more complex than some analyses have

476 previously suggested²¹. We conclude that extreme caution should be exercised when
477 attempting to explain or project local climate-violence relationships on the basis of a single,
478 generalized theory. Large scale cross-sectional studies can be useful for identifying general
479 associations and trends, but an appropriately scaled and structured analysis is required to
480 explain and, potentially, address climate-violence risk factors in geographic context.

481 **Acknowledgment**

482 Authors thank C. Helman for helping to organize the data for the analyses, A. Mussery for
483 helping to organize the SEMs results in the SM, and two anonymous reviewers for insightful
484 comments. D.H. is a USA-Israel Fulbright Fellow for 2018/2019. C.F. is supported by the US
485 Geological Survey Drivers of Drought program and the US Agency for International
486 Development's Famine Early Warning Systems Network.

487 **References**

- 488 1. Scheffran, J., Brzoska, M., Kominek, J., Link, P. M. & Schilling, J. Climate change
489 and violent conflict. *Science (80-)*. **336**, 869–871 (2012).
- 490 2. Hsiang, S. M., Meng, K. C. & Cane, M. A. Civil conflicts are associated with the
491 global climate. *Nature* **476**, 438–441 (2011).
- 492 3. Bernauer, T., Böhmelt, T. & Koubi, V. Environmental changes and violent conflict.
493 *Environ. Res. Lett.* **7**, 15601 (2012).
- 494 4. Koubi, V. Climate Change and Conflict. *Annu. Rev. Polit. Sci.* **22**, 343–360 (2019).
- 495 5. Koubi, V. Climate Change, the Economy, and Conflict. *Curr. Clim. Chang. Reports* **3**,
496 200–209 (2017).
- 497 6. Hodler, R. & Raschky, P. A. Economic shocks and civil conflict at the regional level.
498 *Econ. Lett.* **124**, 530–533 (2014).
- 499 7. Dube, O. & Vargas, J. F. Commodity Price Shocks and Civil Conflict: Evidence from
500 Colombia. *Rev. Econ. Stud.* **80**, 1384–1421 (2013).
- 501 8. Harris, G. & Vermaak, C. Economic inequality as a source of interpersonal violence:
502 Evidence from Sub-Saharan Africa and South Africa. *South African Journal of*
503 *Economic and Management Sciences* **18**, 45–57 (2015).
- 504 9. Zhang, D. D. *et al.* The causality analysis of climate change and large-scale human
505 crisis. *Proc. Natl. Acad. Sci.* **108**, 17296 LP – 17301 (2011).
- 506 10. Carleton, T. A. & Hsiang, S. M. Social and economic impacts of climate. *Science (80)*.
507 **353**, (2016).
- 508 11. Fjelde, H. & von Uexkull, N. Climate triggers: rainfall anomalies, vulnerability and
509 communal conflict in sub-Saharan Africa. *Polit. Geogr.*, 31:444–453, (2012).
- 510 12. Wischnath, G. & Buhaug, H. Rice or riots: On food production and conflict severity
511 across India. *Polit. Geogr.*, 43, 6-15, (2014).
- 512 13. Salehyan, I. & Hendrix C. S. Climate shocks and political violence. *Glob Environ*
513 *Change* 28:239–250, (2014).
- 514 14. Witsenburg, K. M. & Adano, W. R. Of rain and raids: violent livestock raiding in
515 Northern Kenya. *Civil Wars* 11:514–538, (2009).
- 516 15. Raleigh, C. & Kniveton, D. Come rain or shine: An analysis of conflict and climate

- 517 variability in East Africa. *J. Peace Res.*, 49(1), 51-64, (2012).
- 518 16. Nordkvelle, J., Rustad, S. A. & Salmivalli, M. Identifying the effect of climate
519 variability on communal conflict through randomization. *Clim. Change*, 141(4), 627-
520 639, (2017).
- 521 17. Dewart, C. N., Anderson, C. A. & Bushman, B. J. The general aggression model:
522 Theoretical extensions to violence. *Psychol. Violence* **1**, 245–258 (2011).
- 523 18. Cohen, L. E. & Felson, M. Social change and crime rate trends : A Routine Activity
524 Approach. *Am. Sociol. Rev.* **44**, 588–608 (1979).
- 525 19. O’Loughlin, J., Linke, A. M. & Witmer, F. D. W. Effects of temperature and
526 precipitation variability on the risk of violence in sub-Saharan Africa, 1980-2012.
527 *Proc. Natl. Acad. Sci. U. S. A.* **111**, 16712–16717 (2014).
- 528 20. O’Loughlin, J. *et al.* Climate variability and conflict risk in East Africa, 1990–2009.
529 *Proc. Natl. Acad. Sci.* **109**, 18344–18349 (2012).
- 530 21. Hsiang, S. M., Burke, M. & Miguel, E. Quantifying the influence of climate on human
531 conflict. *Science (80-.)*. **341**, (2013).
- 532 22. Hsiang, S. M. & Burke, M. Climate, conflict, and social stability: what does the
533 evidence say? *Clim. Change* **123**, 39–55 (2014).
- 534 23. Helman, D. & Zaitchik, B. F. Temperature anomalies affect violent conflicts in
535 African and Middle Eastern warm regions. *Glob Environ Chang.* (2020).
- 536 24. Ide, T. Research methods for exploring the links between climate change and conflict.
537 *Wiley Interdiscip. Rev. Clim. Chang.* **8**, (2017).
- 538 25. Buhaug, H. Climate not to blame for African civil wars. *Proc. Natl. Acad. Sci. U. S. A.*
539 **107**, 16477–16482 (2010).
- 540 26. Adams, C., Ide, T., Barnett, J. & Detges, A. Sampling bias in climate-conflict research.
541 *Nat. Clim. Chang.* **8**, 200–203 (2018).
- 542 27. Buhaug, H. *et al.* One effect to rule them all? A comment on climate and conflict.
543 *Clim. Change* **127**, 391–397 (2014).
- 544 28. Mach, K. J. *et al.* Climate as a risk factor for armed conflict. *Nature* **571**, 193–197
545 (2019).
- 546 29. Sundberg, R. & Melander, E. Introducing the UCDP georeferenced event dataset. *J.*
547 *Peace Res.* **50**, 523–532 (2013).
- 548 30. Chou, C.-P. & Bentler, P. M. Estimates and tests in structural equation modeling. in
549 *Structural equation modeling: Concepts, issues, and applications*. 37–55 (Sage
550 Publications, Inc, 1995).
- 551 31. Sundberg, R. & Croicu, M. UCDP Non-State Conflict Codebook Version 18.1.
552 *Uppsala Confl. Data Progr. Web Page* 1–10 (2017).
- 553 32. Carpenter, T. G. Tangled web: The Syrian civil war and its implications. *Mediterr. Q.*
554 **24**, 1–11 (2013).
- 555 33. Funk, C. *et al.* A high-resolution 1983–2016 Tmax climate data record based on
556 infrared temperatures and stations by the climate hazard center. *J. Clim.* **32**, 5639–
557 5658 (2019).
- 558 34. Funk, C. *et al.* The climate hazards infrared precipitation with stations—a new

- 559 environmental record for monitoring extremes. *Sci. Data* **2**, 150066 (2015).
- 560 35. Dinku, T. *et al.* Validation of the CHIRPS satellite rainfall estimates over eastern
561 Africa. *Q. J. R. Meteorol. Soc.* **144**, 292–312 (2018).
- 562 36. Maidment, R. I., Allan, R. P. & Black, E. Recent observed and simulated changes in
563 precipitation over Africa. *Geophys. Res. Lett.* **42**, 8155–8164 (2015).
- 564 37. Center for International Earth Science Information Network. - CIESIN - Columbia
565 University. 1999. Poverty Mapping Project: Global Subnational Infant Mortality
566 Rates. Palisades, NY: NASA Socioeconomic Data and Applications Center (SEDAC)
567 [Accessed: 17 February 2019]. Available at: <https://doi.org/10.7927/H4PZ56R2>.
- 568 38. Von Uexkull, N., Croicu, M., Fjelde, H. & Buhaug, H. Civil conflict sensitivity to
569 growing-season drought. *Proc. Natl. Acad. Sci. U. S. A.* **113**, 12391–12396 (2016).
- 570 39. ESA: *Land Cover CCI Product User Guide Version 2.0* [Last access: 17 June 2019].
571 (2019).
- 572 40. Liu, X. *et al.* Comparison of country-level cropland areas between ESA-CCI land
573 cover maps and FAOSTAT data. *Int. J. Remote Sens.* **39**, 6631–6645 (2018).
- 574 41. Didan, K. *et al.* *Multi-Sensor Vegetation Index and Phenology Earth Science Data
575 Records Algorithm Theoretical Basis Document And User Guide Version 4.0.* (2015).
- 576 42. Jiang, Z., Huete, A. R., Didan, K. & Miura, T. Development of a two-band enhanced
577 vegetation index without a blue band. *Remote Sens. Environ.* **112**, 3833–3845 (2008).
- 578 43. Huete, A. *et al.* Overview of the radiometric and biophysical performance of the
579 MODIS vegetation indices. *Remote Sens. Environ.* **83**, 195–213 (2002).
- 580 44. Huang, X., Xiao, J. & Ma, M. Evaluating the Performance of Satellite-Derived
581 Vegetation Indices for Estimating Gross Primary Productivity Using FLUXNET
582 Observations across the Globe. *Remote Sensing* **11**, (2019).
- 583 45. Helman, D., Mussery, A., Lensky, I. M. & Leu, S. Detecting changes in biomass
584 productivity in a different land management regimes in drylands using satellite-derived
585 vegetation index. *Soil Use Manag.* **30**, (2014).
- 586 46. Helman, D., Lensky, I. M., Mussery, A. & Leu, S. Rehabilitating degraded drylands by
587 creating woodland islets: Assessing long-term effects on aboveground productivity and
588 soil fertility. *Agric. For. Meteorol.* **195–196**, (2014).
- 589 47. Helman, D. Land surface phenology: What do we really ‘see’ from space? *Sci. Total
590 Environ.* **618**, 665–673 (2018).
- 591 48. Gitelson, A. A. *et al.* Relationship between gross primary production and chlorophyll
592 content in crops: Implications for the synoptic monitoring of vegetation productivity.
593 *J. Geophys. Res. Atmos.* **111**, (2006).
- 594 49. FAO. Production Database. Crops Dataset. Latest update: November 2016 [Accessed:
595 18 June 2019].
- 596 50. NOAA. Defense Meteorological Satellite Program (DMSP)—Data Archive, Research,
597 and Products [Internet] Earth Observation Group, Boulder [cited 2020]. Available at:
598 <http://ngdc.noaa.gov/eog/dmsp.html>.
- 599 51. Levin, N., Ali, S. & Crandall, D. Utilizing remote sensing and big data to quantify
600 conflict intensity: The Arab Spring as a case study. *Appl. Geogr.* **94**, 1–17 (2018).

- 601 52. Ivan, K., Holobăcă, I.-H., Benedek, J. & Török, I. Potential of Night-Time Lights to
602 Measure Regional Inequality. *Remote Sensing* **12**, (2020).
- 603 53. Bagan, H., Borjigin, H. & Yamagata, Y. Assessing nighttime lights for mapping the
604 urban areas of 50 cities across the globe. *Environ. Plan. B Urban Anal. City Sci.* **46**,
605 1097–1114 (2018).
- 606 54. Li, S., Zhang, T., Yang, Z., Li, X. & Xu, H. Night Time Light Satellite Data for
607 Evaluating the Socioeconomics in Central Asia. *ISPRS - Int. Arch. Photogramm.*
608 *Remote Sens. Spat. Inf. Sci.* **42W7**, 1237–1243 (2017).
- 609 55. Proville, J., Zavala-Araiza, D. & Wagner, G. Night-time lights: A global, long term
610 look at links to socio-economic trends. *PLoS One* **12**, 1–12 (2017).
- 611 56. Stevens, F. R., Gaughan, A. E., Linard, C. & Tatem, A. J. Disaggregating census data
612 for population mapping using Random forests with remotely-sensed and ancillary data.
613 *PLoS One* **10**, 1–22 (2015).
- 614 57. Kumar, S. V *et al.* Land information system: An interoperable framework for high
615 resolution land surface modeling. *Environ. Model. Softw.* **21**, 1402–1415 (2006).
- 616 58. Niu, G.-Y. *et al.* The community Noah land surface model with multiparameterization
617 options (Noah-MP): 1. Model description and evaluation with local-scale
618 measurements. *J. Geophys. Res. Atmos.* **116**, (2011).
- 619 59. Getirana, A. C. V *et al.* The Hydrological Modeling and Analysis Platform (HyMAP):
620 Evaluation in the Amazon Basin. *J. Hydrometeorol.* **13**, 1641–1665 (2012).
- 621 60. Gelaro, R. *et al.* The Modern-Era Retrospective Analysis for Research and
622 Applications, Version 2 (MERRA-2). *J. Clim.* **30**, 5419–5454 (2017).
- 623 61. Hegre, H. & Sambanis, N. Sensitivity analysis of empirical results on civil war onset.
624 *J. Conflict Resolut.* **50**, 508–535 (2006).
- 625 62. Baron, R. A. & Ransberger, V. M. Ambient temperature and the occurrence of
626 collective violence: The ‘long, hot summer’ revisited. *Journal of Personality and*
627 *Social Psychology* **36**, 351–360 (1978).
- 628 63. Bell, P. A. & Baron, R. A. Aggression and Heat: The Mediating Role of Negative
629 Affect1. *J. Appl. Soc. Psychol.* **6**, 18–30 (1976).
- 630 64. Baron, R. A. Aggression as a function of ambient temperature and prior anger arousal.
631 *Journal of Personality and Social Psychology* **21**, 183–189 (1972).
- 632 65. Baron, R. A. & Bell, P. A. Aggression and heat: The influence of ambient temperature,
633 negative affect, and a cooling drink on physical aggression. *J. Pers. Soc. Psychol.* **33**,
634 245–255 (1976).
- 635 66. Anderson, C. A. Temperature and Aggression: Ubiquitous Effects of Heat on
636 Occurrence of Human Violence. *Psychol. Bull.* **106**, 74–96 (1989).
- 637 67. Amine, B. M. & Fatima, B. Determinants of on-farm diversification among rural
638 households: Empirical evidence from Northern Algeria. *International Journal of Food*
639 *and Agricultural Economics (IJFAEC)* **04**, 87–99
- 640 68. Keita, K. Conflict and conflict resolution in the Sahel: The Tuareg insurgency in Mali.
641 *Small Wars Insur.* **9**, 102–128 (1998).
- 642 69. Bächler, G. *Violence through environmental discrimination: Causes, Rwanda arena,*

- 643 *and conflict model. 2*, (Kluwer Academic, 1998).
- 644 70 Buhaug, H. Climate–conflict research: some reflections on the way forward. *Wiley*
- 645 *Interdisciplinary Reviews: Climate Change*, 6(3), 269-275 (2015).